Formation of silver nanoparticles inside a soda-lime glass matrix in the presence of a high intensity Ar+ laser beam

M. D. Niry, J. Mostafavi-Amjad, H. R. Khalesifard, A. Ahangary, and Y. Azizian-Kalandaragh

Citation: J. Appl. Phys. **111**, 033111 (2012); doi: 10.1063/1.3684552
View online: http://dx.doi.org/10.1063/1.3684552
View Table of Contents: http://jap.aip.org/resource/1/JAPIAU/v111/i3
Published by the American Institute of Physics.

Formation of silver nanoparticles inside a soda-lime glass matrix in the presence of a high intensity Ar^+ laser beam

M. D. Niry,[1,2,a)] J. Mostafavi-Amjad,[1] H. R. Khalesifard,[1,2,b)] A. Ahangary,[1] and Y. Azizian-Kalandaragh[1,3,c)]
[1]*Department of Physics, Institute for Advanced Studies in Basic Sciences (IASBS), Zanjan 45137-66731, Iran*
[2]*Optics Research Center, Institute for Advanced Studies in Basic Sciences (IASBS), Zanjan 45137-66731, Iran*
[3]*Department of Physics, University of Mohaghegh Ardabili (UMA), P.O. Box 179, Ardabil, Iran*

(Received 19 November 2011; accepted 11 January 2012; published online 15 February 2012)

Formation and motion of the silver nanoparticles inside an ion-exchanged soda-lime glass in the presence of a focused high intensity continuous wave Ar^+ laser beam (intensity: 9.2×10^4 W/cm^2) have been studied in here. One-dimensional diffusion equation has been used to model the diffusion of the silver ions into the glass matrix, and a two-dimensional reverse diffusion model has been introduced to explain the motion of the silver clusters and their migration toward the glass surface in the presence of the laser beam. The results of the mentioned models were in agreement with our measurements on thickness of the ion-exchange layer by means of optical microscopy and recorded morphology of the glass surface around the laser beam axis by using a Mirau interferometer. SEM micrographs were used to extract the size distribution of the migrated silver particles over the glass surface. © *2012 American Institute of Physics*. [doi:10.1063/1.3684552]

I. INTRODUCTION

Size has significant effect on the physical properties of nanoparticles.[1–3] This is due to non-zero number-ratio of surface to bulk atoms and strong variation of this ratio versus the particle diameter.[3] Decreasing the particle size increases contribution of the surface atoms in the physical properties of the particle.[4]

Very fast nonlinear optical response of metal nanoparticles makes them a proper choice in construction and design of optoelectronic devices, optical sensors, and switches.[5] Glass matrices doped with metal nanoparticles have significant nonlinear optical properties.[6–11] In addition, between metals, silver has the highest optical skin depth, in the range of 10-100 μm, in the visible spectrum, which increases to 1 mm if one moves into the near-infrared telecommunication band (i.e., $\lambda \sim 1.5$ μm).[12] This property makes silver clusters a proper choice for surface plasmon–based components,[13–15] where their sizes easily can be less than the electromagnetic wave skin depth.

Many methods have been used to produce silver nanoparticles,[16–20] many of them describing construction of silver nanoparticles in solutions, like chemical reduction techniques.[21] Some of them are concerned with formation of silver nanoparticles in matrices, like soda-lime glasses.[6–8] For example, thermal annealing of Ag^+/Na^+ ion-exchanged (IE) glasses in H_2 atmosphere cause the silver ions to reduce, aggregate, and form silver clusters inside the glass matrix where the ion-exchange process has taken place.[22] Also, it is possible that, by redistribution of the alkali ions inside the IE glass matrix, charge compensation phenomena occurs and Ag^+ ions reduce to Ag atoms.[23] But to produce the silver nanoparticles, we irradiated an ion-exchanged glass surface by a high power Ar^+ laser beam.[6,7] The laser beam interacts with the glass and reduces the silver ions inside the glass matrix. It has been suggested that the non-bridging oxygens (NBO) inside the glass matrix can provide the required electrons through the following reaction:[23,24]

$$Ag^+ + NBO \rightarrow Ag^0 + NBO^+. \quad (1)$$

Absorption of the laser beam power may cause the temperature of the IE glass to pass over the glass transition temperature. Silver atoms diffuse inside the glass matrix, aggregate, and can form nano-sized silver clusters, where the matrix is almost soft in such a high temperature. During interaction of the laser beam and the IE glass, nano-silver particles migrate to the glass surface, where the surface tension prevents them to diffuse back into the glass matrix, and they only diffuse over the glass surface, like 2-dimensional random walkers.

In the rest of this manuscript, we will discuss the formation procedure of the silver particles and will explain how they diffuse inside the glass matrix during the interaction process. In Sec. II, the experiments and some of the obtained results have been presented. In Sec. III, the ion-exchange process is modeled as a simple one-dimensional diffusion process. In Sec. IV, by considering a Gaussian profile for the focused Ar^+ laser beam, the spatial profile of temperature and viscosity inside the interaction area have been studied. In Sec. V, a reverse diffusion process model has been used to explain the migration of the silver clusters toward the glass surface, where silver nanoparticles are aggregated, and at last, Sec. VI is devoted to discussion of the results of this work.

[a)]Author to whom correspondence should be addressed. Electronic mail: m.d.niry@iasbs.ac.ir. URL: http://www.iasbs.ac.ir/~m.d.niry.
[b)]Electronic mail: khalesi@iasbs.ac.ir.
[c)]While our team was working on this project, Y. Azizian-Kalandaragh was with the physics department of IASBS, and now he is a member of the physics department of UMA.

TABLE I. Result of wet chemical analysis of the soda-lime glass slides used on our experiments.

Compound	Weight percent
SiO_2	80
CaO	9.41
Na_2O	4
MgO	3.3
Al_2O_3	2.2
K_2O	0.41
S	0.2
Fe_2O_3	0.11
P_2O_5	0.11
Total	99.74

II. EXPERIMENTS

During the experiments, the well-known Ag^+/Na^+ ion-exchange technique has been used to prepare the required samples.[25–27] Soda-lime glass slides of dimensions 39 mm × 25 mm × 0.85 mm have been merged into a molten mixture of $NaNO_3/AgNO_3$ (96/4 W%) at 420 °C for 4 h. Table I shows the results of wet chemical analysis of the glass slide. The IE samples were irradiated by a focused Ar^+ laser beam (wavelength: 514 nm; power: 2.3 W; focus point diameter: 40 μm) for 60 s.

Structure investigations of the clusters formed over the glass surface were performed using a scanning electron microscope (SEM; LEO, Model: 1430VP) at 15 kV accelerating voltages (Fig. 1).

Optical absorption spectra of the sample before and after interaction with the laser beam have been recorded by using an UV-visible-near-infrared (UV-Vis-NIR) spectrophotometer (SPM; Varian, Model: Cary 5E) in the wavelength range of 385 to 800 nm (Fig. 2). The spectra are recorded from the circular area C_i (radius = 10 μm) in Fig. 1. To record the optical absorption spectra of such a small area, we have modified the sample holder of the SPM. A 10 × microscope objective has been installed in front and another one behind the sample, where the latter focuses the impinging light over the sample and the former collimates the transmitted light through the sample toward the detection unit of the SPM. It should be mentioned, doing the ion-exchange process for 4 h at 420 °C may cause some of the Ag^+ ions to reduce to Ag atoms by a different mechanism, like the existence of some trace amount of FeO that can provide the required electron to reduce the Ag^+, and then Fe_2O_3 will form.[28] Also we guess that, at this temperature, the silver atoms are mobile enough to aggregate and form clusters. This is why, in Fig. 2, even just after the ion-exchange process, a peak has appeared around 420 nm on the absorption spectra of the sample. The peak corresponds to the surface plasmon resonance of the silver nanoparticles.[28] After interaction with the laser beam, the surface plasmon resonance became stronger. Absorption spectra of C_1 and C_2 areas (of Fig. 1, centered at 20 and 40 μm from the center of the interaction region, respectively) depict the formation of silver clusters. Surface plasmon resonances for the particles in the C_1 (C_2) area mostly occurred around 423 (435) nm. The larger area under the surface plasmon resonance peak for C_1 in respect to the C_2 region is an indication for a larger amount of silver particles, and its blueshift in respect to C_2 can be assigned to the smaller size of the particles in this region.[9,23,28]

Figures 3(a)–3(d) are the optical micrographs of the interaction region, where the microscope (Olympus, Model: IX71) is focused just on the surface of the glass slide [Figs. 3(a) and 3(c)] and 4 μm under it [Figs. 3(b) and 3(d)]. Figures 3(a) and 3(c) show that a considerable population of silver clusters is formed over the glass surface, but some smaller population of them are in the center of the interaction region in Fig. 3(b) and 3(d) (i.e., 4 μm under the glass surface). Someone may doubt that the glass surface is concave and all of the silver clusters are over the glass surface.

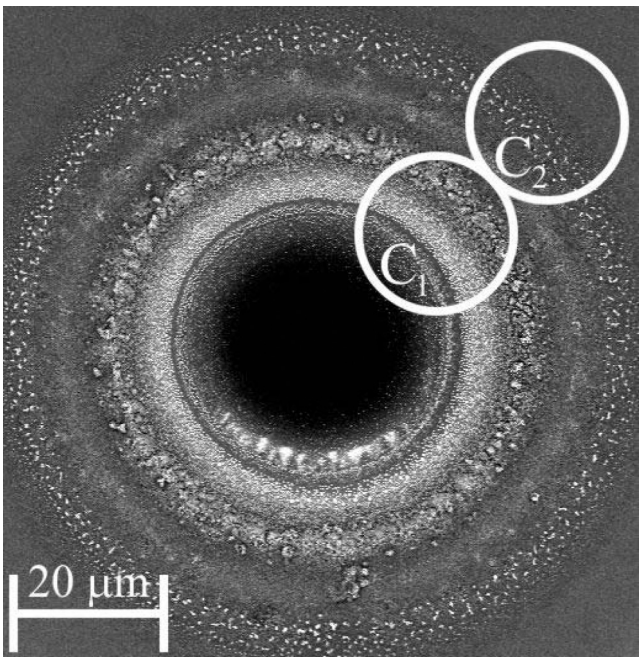

FIG. 1. SEM micrograph of the interaction area; nano-silver particles aggregated over the glass surface. The optical absorption spectra are recorded from the circular area C_i; results are shown in Fig. 2.

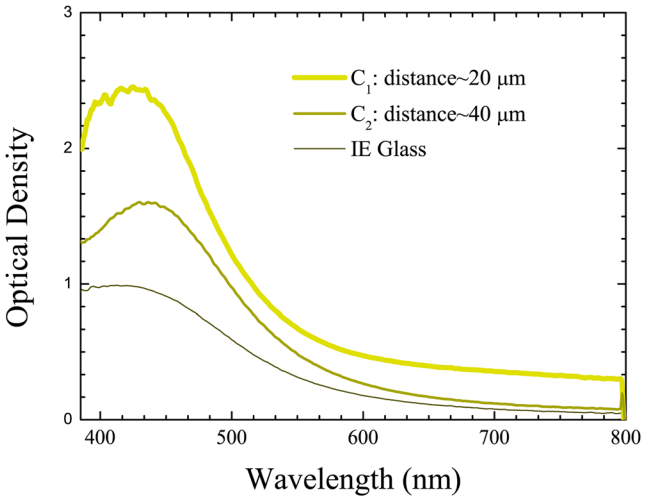

FIG. 2. (Color online) Optical absorption spectra of the IE glass sample before and after interaction with Ar^+ laser beam. The spectra have been recorded, referenced to the soda-lime glass slide.

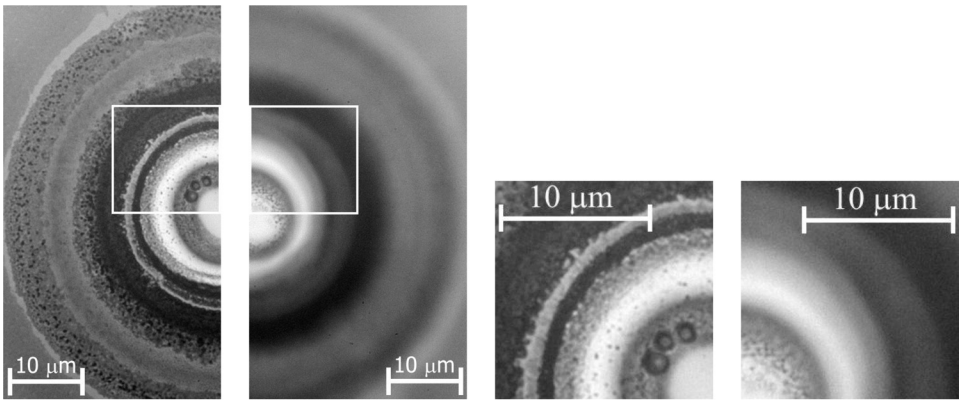

FIG. 3. Optical micrographs. (a) and (b) The microscope is focused on the surface and 4 μm under the surface of the glass slide. (c) and (d) Part of the image in white boxes in (a) and (b), respectively.

Therefore, the Mirau interferometry technique[29–34] has been used to investigate the morphology of the interaction region. A 10 × Mirau objective (Nikon, Model: CF IC Epi Plan DI) in combination with a piezoelectric actuator (Physik Instrumente, Model: P-750.20) and the optical microscope have been used to make a Mirau interferometer. The interferometer had 10 nm (100 nm) resolution along (perpendicular to) the optical axis of the objective. Figure 4 shows the result of this measurement. As this figure shows, the glass surface after the interaction would not be flat anymore, but a bump of about 400 nm was formed at the center of the interaction region.[35,36] One can see that, for distances larger than 10 μm from the center of the interaction area, the surface fluctuations are ± 10 nm and the glass surface is almost flat.

Also, we developed a code for statistical analysis of the size distribution of the silver clusters over the glass surface that can be observed in SEM micrographs. The probability density function (PDF) for diameters of the silver particles inscribed inside the rectangle S in Fig. 5(a) is shown in Fig. 5(b). The PDF indicates an average value of 90 nm and variance of 31 nm for diameters of the particles.

To find the depth of the IE layer over the glass sample, the glass slide has been cut in stripes of $w_s \sim 15$ mm in width and polished through the cut sides. Then, the IE layer has been monitored by the optical microscope, where it was equipped with its phase contrast accessories (Fig. 6). As it can be seen, the half value layer (HVL) of the IE layer is approximately 55 μm (Figs. 6 and 7).

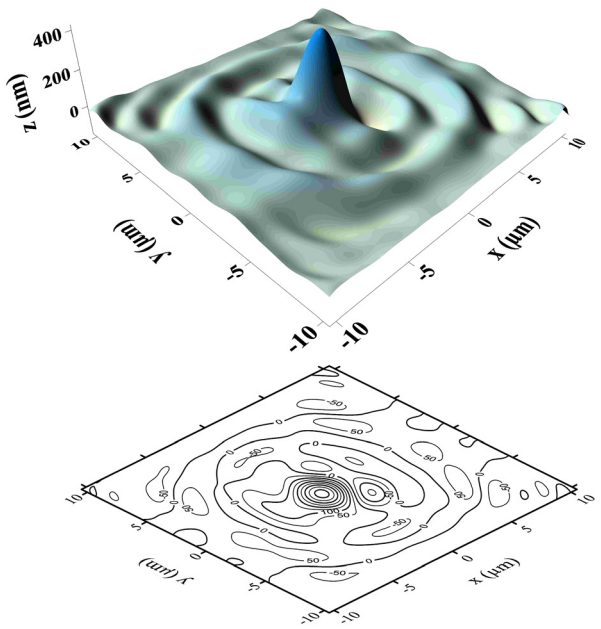

FIG. 4. (Color online) Morphology of the interaction region of the laser-irradiated IE glass measured by Mirau interferometry technique.

III. DIFFUSION OF SILVER IONS INSIDE THE GLASS MATRIX

To explain the diffusion of Ag^+ ions inside the glass matrix, a simple one-dimensional diffusion model is considered, where the glass matrix fills the half-space $z = 0$ to $+\infty$. In this case, the concentration of silver ions inside the glass matrix $c(z, t)$ can be explained by a complementary error function, erfc (1 minus error function)[27] (Fig. 7),

$$c(z, t) = c_0 \mathrm{erfc}\left(\frac{z}{\sqrt{4Dt_d}}\right), \tag{2}$$

where D, t_d, and c_0 are the diffusion coefficient of silver ions inside the glass matrix at the ion-exchange temperature, duration time of the ion-exchange process, and concentration of the silver ions over the glass surface, respectively. According to the Arrhenius law, the diffusion coefficient for absolute temperatures, T, that are lower than the glass transition temperature can be written as

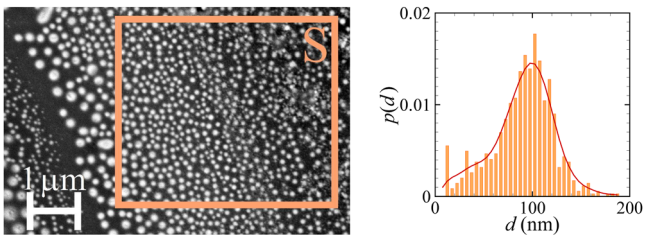

FIG. 5. (Color online) (a) SEM micrograph of silver nanoparticles over the IE glass surface after the interaction. (b) Probability density function for diameter of the particles inscribed inside the rectangle S.

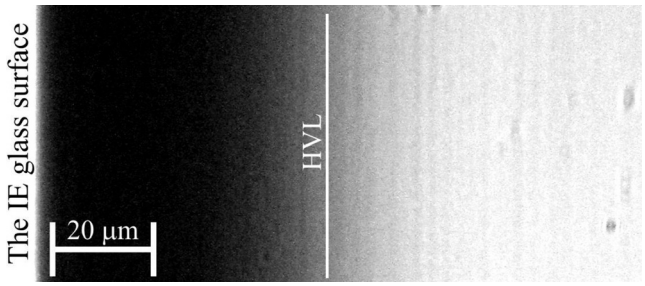

FIG. 6. X-section of the IE layer; optical micrograph. The HVL of the IE layer after 4 h is approximately 55 μm.

$$D(T) = D_0 e^{-\varepsilon_a/RT}, \tag{3}$$

where ε_a is the activation energy of the diffusion process and R is the ideal gas constant.[37] Referring to the result reported by Stewart[37] for typical soda-lime glasses at the temperature range 315–373 °C, $D_0 = 1.59 \times 10^{-7}$ m^2/s and $\varepsilon_a = 9.1 \times 10^4$ J/mole. So, one can estimate the diffusion coefficient at 420 °C as $D = 2.20 \times 10^{-14}$ m^2/s. In a one-dimensional Brownian diffusion problem, the diffusion length Δz can be estimated by[38]

$$\langle (\Delta z)^2 \rangle = 2Dt_d, \tag{4}$$

where $\langle \ldots \rangle$ represents the ensemble average. According to Eq. (4), the effective thickness of the IE layer, Δz, is approximately 25 μm (Fig. 7). But when one is looking through the sample perpendicular to the z-axis, the concentration of the silver ions in the IE layer or the optical density of the sample will be integrated along the mentioned axis. This is why Fig. 6 shows the HVL of about 55 μm.

Knowing the overall diffusion direction of the silver ions through the glass matrix, one can consider an absorption coefficient α for the IE glass that, in the first order of approximation, is a linear function of $c(z)$,[39]

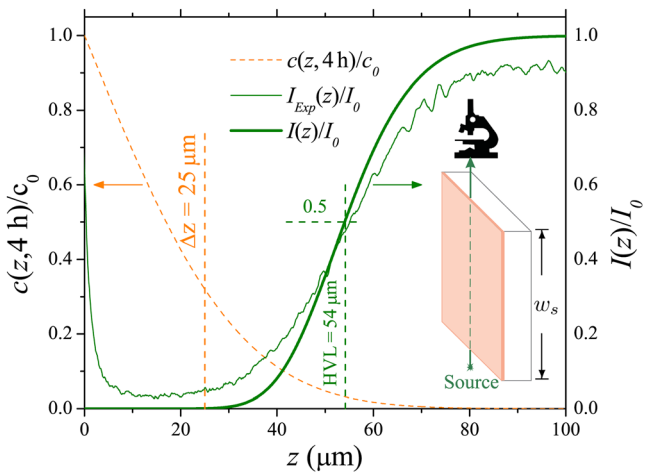

FIG. 7. (Color online) Dashed curve shows the normalized concentration of silver ion in the IE glass. The effective thickness of the IE-layer after 4 h is approximately 25 μm [Eq. (4)]. Solid thick and thin curves show calculated [Eq. (6)] and experimental results for normalized intensity of the light passed along the IE-layer of the glass slide, respectively. Experimental data extracted from Fig. 6. The inset shows the schematic setup has been used to obtain Fig. 6.

$$\alpha(c) = \varepsilon c(z), \tag{5}$$

where ε is the molar absorptivity.

Now, using the Beer-Lambert law for an impinging light of intensity $\mathcal{I}_0$, one can estimate the transmitted intensity, $I(z)$, along an axis perpendicular to the z-axis and through an IE glass stripe of width w_s as

$$I(z) = \mathcal{I}_0 e^{-\varepsilon c(z) w_s}. \tag{6}$$

Fitting Eq. (6) to the variations of gray scale density of Fig. 6, ε will be obtained as ~15 cm^{-1}. Figure 7 shows the results of this calculation for w_s = 15 mm.

The intensity of a focused Gaussian beam around the focus point and for propagation distances, z, much less than the confocal parameter of the Gaussian beam can be written as[40,41]

$$I(r, z) = I_0 e^{-2(r/w_0)^2} e^{-\overline{\alpha} z}, \tag{7}$$

where I_0 is the axial intensity of the focused Gaussian laser beam at $z = 0$ (i.e., glass surface) and $\overline{\alpha}$, the mean value of the IE layer absorption coefficient. Considering the laser beam minimum waist, w_0 ~20 μm, and its power, P, then $I_0 = 2P/(\pi w_0^2)$. Also, since the 25-μm-thick IE layer is much thinner than the 300 μm confocal parameter of the Gaussian beam, then Eq. (7) well describes the behavior of the focused Ar^+ laser beam when it is crossing the IE layer. The last term in Eq. (7) that is taken from the Beer-Lambert law represents the average amounts of dissipated energy in the medium. $\overline{\alpha}$ could be related to ε by using Eqs. (2) and (5), and in our case, for an IE layer of thickness Δz = 25 μm, it was measured as 20 cm^{-1}.

The element of power, p, carried by a Gaussian laser beam through surface element $rd\varphi dr$ is $Ird\varphi dr$. According to the Beer-Lambert law, a differential element of power, dp, dissipated in a differential element of volume of glass, dV, is equal to $\overline{\alpha} p dz$. The dissipation rate of the beam energy per unit volume is represented by $Q = dp/dV$. Therefore, the portion of the beam power dissipated per unit volume, $Q(r, z)$, in the cylindrical coordinates is

$$Q(r, z) = \begin{cases} \overline{\alpha} I_0 e^{-\overline{\alpha} z - 2(r/w_0)^2} & : \ 0 < z \le \Delta z, \\ 0 & : \ z > \Delta z. \end{cases} \tag{8}$$

In writing Eq. (8), it is considered that the laser beam absorption for those parts of the glass matrix that are below the IE layer is negligible.

IV. HEAT EQUATION

To find the space and time-dependent temperature profile, $T(\mathbf{r}, t)$, inside the glass matrix while the laser beam is interacting with the medium, the heat equation,

$$\rho c_p \frac{\partial T(r, z, t)}{\partial t} = \nabla.(k(T)\nabla T) + Q(r, z), \tag{9}$$

should be solved,[42,43] where T, ρ, c_p, and k are the temperature, glass density, specific heat capacity, and temperature-dependent thermal conductivity, respectively. Considering

the room temperature values of these parameters for a typical soda-lime glass,[39,44] $\rho \simeq 2.52\ gr/cm^3$, $c_p \simeq 0.84 J/(gr.K)$, $k \simeq 1.25 W/(m.K)$, and $T = 27\,^{\circ}\mathrm{C}$, the thermal diffusivity $\kappa = k/(c_p\rho)$ can be calculated as $6 \times 10^5\ \mu m^2/s$. This large value for κ allows us to consider a stationary (i.e., $t \gg w_0^2/\kappa$) solution for Eq. (9) in the interaction area of radius $w_0 = 20\ \mu m$. Since k is highly temperature dependent [see the Appendix for calculation of $k(T)$], to solve Eq. (9) at the interaction temperature we used an iterative technique, starting from the room temperature conditions. It should be mentioned that the solution obtained from the iteration procedure should converge to a stationary solution. Considering the arrangement of the experiments, the following boundary conditions (BC) should be applied to solve the heat equation [Eq. (9)]:

• BC #1: We define a specific radius, R, for which one can write

$$\forall z, t : T(r \geq R, z, t) = T_\infty = 27\,^{\circ}\mathrm{C}. \tag{10}$$

In order to have an exact solution for Eq. (9), R should get close to infinity, but the simulation cost and precision of the solution should be balanced, so we select $R = 5$ mm, which is quite larger than the radius of the interaction area ($w_0 = 20\ \mu m$).

• BC #2: Lower and upper interfaces of the glass slide cool down by air convection and radiation,[39,45,46] but the rate of heat transfer through each surface is negligible, so

$$\left.\frac{\partial T}{\partial z}\right|_{z=0,\,b} = 0, \tag{11}$$

where b is the thickness of the glass slide.

Now, using the mentioned iteration technique, BC #1 and BC #2, the heat transfer equation is solved for a glass disk of radius $R \sim 5$ mm and thickness $b \sim 0.85$ mm by finite elements method (FEM) implementation in COMSOL Multiphysics.[47] Parts of the numeric result obtained for the temperature profile inside the glass matrix in terms of r and z are shown in Fig. 8(a). It is considered that the laser beam is propagating along the $+z$ direction and focused at $z = 0$ to an area of 40 μm in diameter. Combining these results and the temperature-dependent viscosity formula for a typical soda-lime glass,[44]

$$\log_{10}(\eta/(\mathrm{Pa.s})) = -2.585 + 4215/(T[^{\circ}\mathrm{C}] - 263), \tag{12}$$

one can find the viscosity profile of the glass around the interaction area while the laser is interacting with it [Fig. 8(b)].

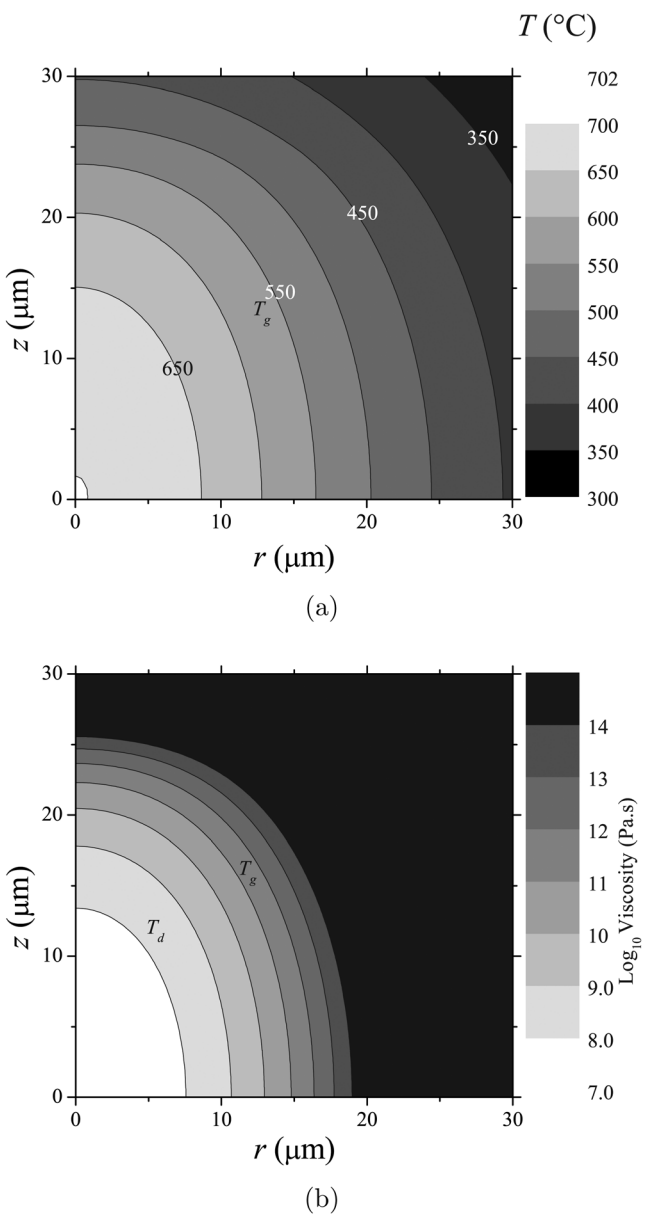

FIG. 8. (a) and (b) Stationary state temperature and viscosity profile of the glass matrix in cylindrical coordinates induced by the laser beam during the interaction. The laser beam coincides with the z-axis. T_g and T_d are glass transition– and dilatometric softening–temperature, respectively (Ref. 44).

V. REVERSE DIFFUSION PROCESS (RDP) MODEL

Figures 1 and 3(a)–3(d) show silver nano- and micro-clusters that are formed over the IE glass surface during interaction with the Ar^+ laser beam. To explain this phenomena, a reverse diffusion model for motion of the silver atoms inside the softened glass matrix is introduced in here. It should be mentioned that the high intensity laser beam can increase the temperature of the interaction area up to $\sim 700\,^{\circ}\mathrm{C}$ [Fig. 8(a)]. Referring to Eq. (3), the diffusion coefficient of the silver atoms has a profile that its maximum value is $\sim 2\ \mu m^2/s$ on the beam axis and over the glass surface. This value decreases to $D(500\,^{\circ}\mathrm{C} \sim 0.1\ \mu m^2/s$ ($D(T_\infty) \sim 0.03\ pm^2/s$) around the interaction area and in the depth of the glass matrix, where the glass temperature is getting close to the ambient temperature. Figure 8(a) shows that, at 15 μm from the center of the interaction area, the temperature decreases down to the glass transition temperature $T_g \sim 570\,^{\circ}\mathrm{C}$. To study the motion of the silver atoms inside such media having a typical viscosity profile as Fig. 8(b), the diffusion equation in the cylindrical coordinates should be rewritten as[27,48]

$$\frac{\partial C}{\partial t} = \nabla.[D(T)\nabla C(r, z, t)], \tag{13}$$

where $C(r, z, t)$ represents the time-dependent concentration of the Ag atoms. $D(T)$ can be found from Eq. (3), and the temperature profile of the interaction area is considered constant during the interaction [Fig. 8(a)]. Equation (13) should be solved subject to the following boundary conditions:

$$C(r, 0, t) = 0, \tag{14a}$$

$$\left.\frac{\partial C(r, z, t)}{\partial z}\right|_{z \to b} = 0, \tag{14b}$$

$$\left.\frac{\partial C(r, z, t)}{\partial r}\right|_{r \to R} = 0. \tag{14c}$$

In writing Eq. (14a), it is supposed that all the silver atoms, which are diffused out of the glass matrix and formed silver clusters over the glass surface, will not diffuse back into the glass matrix again. The initial value of C in Eq. (13) can be obtained from Eq. (2),

$$C(r, z, 0) = c(z, 4\,\mathrm{h}), \tag{15}$$

$c(z, 4\ \mathrm{h})$ indicates the Ag^+ ion concentration inside the IE glass before the interaction with the laser beam. To solve Eq. (13), we used implementation of FEM in COMSOL.[47]

Figure 9 shows spatial distribution of the normalized concentration of the silver either in ionic or atomic form inside the glass matrix around the laser beam axis, where the sample interacted for 60 s with the Ar^+ laser beam.

VI. DISCUSSION

In this manuscript, the Ag^+/Na^+ ion-exchange between a molten salt and the matrix of a soda-lime glass has been modeled as a simple one-dimensional diffusion process. The results obtained from the model are in considerable agreement with the experimental results, as shown in Figs. 6 and 7. Then, aggregation and formation of silver nanoparticles on the IE soda-lime glass surface have been studied under the interaction of a high intensity Ar^+ laser beam. To explain this phenomena, the temperature profile that has been induced inside the glass matrix by absorption of the laser beam power was calculated according to the heat equation (Sec. IV). Silver atoms that have been reduced by irradiation of the laser beam[23,24] diffuse inside the glass matrix, aggregate, and form nano-sized silver clusters.

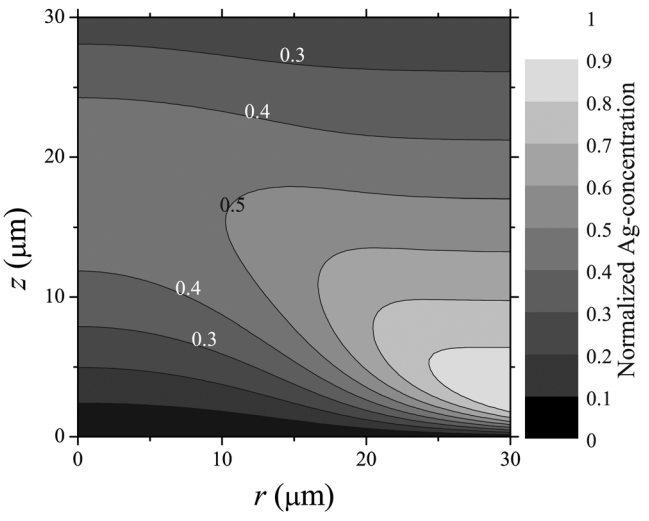

FIG. 9. Normalized spatial concentration of Ag^+, $C(r, z, 60\ \mathrm{s})/c_0$, in cylindrical coordinates, where sample interacted for 60 s with Ar^+ laser beam.

Regarding the high tendency of silver atoms for aggregation and their low diffusion constant inside the glass matrix, most of the nanoparticles should remain inside the glass matrix, but results of optical microscopy show that many of them have migrated toward the surface of the glass [Figs. 3(a) and 3(c)].[23,49] Accurate study of Fig. 8(a) provided some suggestions for introducing a mechanism to explain this behavior. At the focal point of the laser beam, the temperature of the glass matrix can reach up to 700 °C [Fig. 8(a)]. Vollmer *et al.* reported[10] that the silver nanoparticles can be cracked up while interacting with a laser beam (λ = 514 nm, intensity ~10-100 W/cm^2). We expect that, when the silver particles are in high temperature (above the glass transition temperature), this should be done more easily. Considering this and Eq. (7), one can estimate, for distances larger than ~45 μm from the focused point of the laser beam over the glass surface, the intensity of light is low enough ($I < 10$ W/cm^2) to permit the nanoparticles to aggregate and create diffusion- limited aggregation,[6] but around the beam axis, we expect that the silver clusters get close to atoms in size. Between these limits, particles are sorted by their size, where smaller (larger) ones are inside (outside). In other words, we believe that, where the intensity of the laser beam over the surface of the sample is lower, the radiation pressure decreases and the silver atoms can aggregate to make larger particles (one can see this by comparing the surface plasmon resonance peaks in Fig. 2). It should be mentioned that the concentric rings around the interaction area that are free from the particles appeared in coincidence with the diffraction pattern of the microscope objective that focused the laser beam over the sample. The clusters were pushed out of the intense regions of the diffraction pattern and aggregated inside the low intensity parts over the glass surface.[6]

During the interaction of the laser and the IE glass, such small particles are mobile around the beam axis in a typical viscosity profile that is shown in Fig. 8(b). Getting closer to the glass surface, the mobility of silver particles increase. As a result, the particles will have an overall drift toward the glass surface. That is what we called the reverse diffusion process (RDP) in Sec. V. Considering the 700 °C temperature for the glass surface, one can use Eq. (4) to find that the time scale of the RDP is about a minute, which is in good agreement with our experimental observations. When the silver particles reach to the glass surface, the surface tension prevents them to diffuse back into the glass matrix. Such nanoparticles not only should diffuse out of the hot interaction region by the mentioned mechanism, but the radiation pressure of the scattered electromagnetic field of the focused laser beam should also push them out of this region. This is why the center of the interaction area is almost free from the silver particles (Fig. 1).

Referring to Fig. 1, one can estimate the amount of silver particles over the glass surface by considering that they are spheres of average radius of 45 nm [Fig. 5(b)] that are distributed inside a ring of inner (outer) radius of 20 (50) μm. Counting the number of particles in Fig. 5(a), one may take the number density of ~50 particles/μm^2 over the

mentioned ring. This will result in a mass of ~1.0 ng for all silver particles inside the ring. It should be noted that a homogeneous distribution for the particles has been considered here. This is different with Fig. 1 and will cause an overestimation of 10% for the calculated mass. In the other way, referring to Fig. 9, a cylinder of 10 (20) μm in radius (height) in the center of the interaction region should be a source for the silver particles that are migrated over the mentioned ring. Considering a one-to-one exchange for the whole Na^+ ions with Ag^+ ions in this region during the ion-exchange process, ~0.8 ng of Ag is contained in this cylinder, which is in the same order of magnitude as the mass of the Ag particles over the glass surface.

Figure 8 shows that the radius of a region that is heated up to dilatometric softening- temperature, T_d, is ~10 μm. When the temperature of a glass sample goes beyond T_d, its deformation is mostly like a liquid and its dilation will not be sensed any more. This is also in agreement with the observation of morphology of the glass surface around the interaction area that is shown in Fig. 4.

ACKNOWLEDGMENTS

The authors would like to thank SEM Center of the University of Mohaghegh Ardabili provide the laboratorial facilities for recording SEM micrographs.

APPENDIX: THE HEAT CONDUCTIVITY OF SODA-LIME GLASS

To solve the heat equation [Eq. (9)], the heat conductivity of glass in a broad range of temperature is needed. Knowing the phonon conductivity of each of the oxides in the glass composition, the phonon thermal conductivity of glass can be predicted by the following empirical formula:[39]

$$k_c = \sum_i A_i C_i, \tag{A1}$$

where A_i is the phonon thermal conductivity coefficient of component i and C_i is the weight percent of component i. Choudhary and Potter reported A_i values for different oxides that can be found in soda-lime glasses.[39] Using these values for our glass samples, k_c is found as 1.25 W/(m·K). It is known that the thermal conductivity of glass matrix grows exponentially with temperature and can be described as[36]

$$k(T) = k_c e^{\gamma(T-300\,\mathrm{K})}, \tag{A2}$$

where the exponent γ is ~6.7×10^{-4} K^{-1}.

[1]A. Henglein, Chem. Rev. **89**, 1861 (1989).
[2]S. Mann and H. Colfen, Angew. Chem. **115**, 2452 (2003).
[3]N. Ichinose, Y. Ozaki, and S. Kashu, *Superfine Particle Technology* (Springer, New York, 1992).
[4]A. N. Shipway, E. Katz, and I. Willner, ChemPhysChem **1**, 18 (2000).
[5]O. Krichevski, E. Tirosh, and G. Markovich, Langmuir **22**, 867 (2006).
[6]A. Nahal, J. Mostafavi-Amjad, A. Ghods, M. R. H. Khajehpour, S. N. S. Reihani, and M. R. Kolahchi, J. Appl. Phys. **100**, 053503 (2006).
[7]F. Gonella, G. Mattei, P. Mazzoldi, E. Cattaruzza, G. W. Arnold, G. Battaglin, P. Calvelli, R. Polloni, R. Bertoncello, and R. F. Haglund, Appl. Phys. Lett. **69**, 20 (2009).
[8]J. Feng, X. Zhao, B. Liu, and X. Zhou, Opt. Commun. **281**, 5041 (2008).
[9]U. Kreibig and M. Vollmer, *Optical Properties of Metal Clusters* (Springer, New York, 1995).
[10]M. Vollmer, R. Weidenauer, W. Hoheisel, U. Schulte, and F. Träger, Phys. Rev. B **40**, 12509 (1989).
[11]T. C. Chu, W. C. Liu, and D. P. Tsai, Opt. Commun. **246**, 561 (2005).
[12]W. L. Barnes, A. Dereux, and T. W. Ebbesen, Nature **424**, 824 (2003).
[13]H. Mertens, J. Verhoeven, A. Polman, and F. D. Tichelaar, Appl. Phys. Lett. **85**, 1317 (2004).
[14]H. Ditlbacher, A. Hohenau, D. Wagner, U. Kreibig, M. Rogers, F. Hofer, F. R. Aussenegg, and J. R. Krenn, Phys. Rev. Lett. **95**, 257403 (2005).
[15]S. I. Bozhevolnyi, V. S. Volkov, E. Devaux, J.-Y. Laluet, and T. W. Ebbesen, Nature **440**, 508 (2006).
[16]J. M. Köhler, M. Held, U. Hübner, and J. Wagner, Chem. Eng. Technol. **30**, 347 (2007).
[17]S. Behrens, J. Wu, W. Habicht, and E. Unger, Chem. Mater. **16**, 3085 (2004).
[18]S. Kundu, M. Mandal, S. K. Ghosh, and T. Pal, J. Colloid Interface Sci. **272**, 134 (2004).
[19]L. Rodríguez-Sánches, M. C. Blanco, and M. A. López-Quintela, J. Phys. Chem. B **104**, 9683 (2000).
[20]M. A. Villegas, M. A. García, S. E. Paje, and J. LLopis, Mater. Res. Bull. **40**, 1210 (2005).
[21]K. Park, D. Seo, and J. Lee, Colloids Surf., A **351**, 313 (2008).
[22]A. Miotello, G. D. Marchi, G. Mattei, and P. Mazzoldi, Appl. Phys. A **67**, 527 (1998).
[23]A. Miotello, M. Bonelli, G. D. Marchi, G. Mattei, P. Mazzoldi, C. Sada, and F. Gonella, Appl. Phys. Lett. **79**, 2456 (2001).
[24]Y. Kondo, H. Inouye, S. Fujiwara, T. Suzuki, T. Mitsuyu, T. Yoko, and K. Hirao, J. Appl. Phys. **88**, 1244 (2000).
[25]A. Nahal, H. R. M. Khalsifard, and J. Mostafavi-Amjad, Appl. Phys. B **79**, 513 (2004).
[26]A. Nahal and H. R. M. Khalsifard, Opt. Mater. **29**, 987 (2007).
[27]S. I. Najafi, *Introduction to Glass Integrated Optics* (Artech House, Boston, 1992).
[28]A. A. Ahmed and E. W. Abd Allah, J. Am. Ceram. Soc. **78**, 2777 (1995).
[29]T. Doi and T. Kurosawa, Proc. SPIE **5776**, 121 (2005).
[30]J. W. Kang and C. K. Hong, Opt. Eng. **46**, 040506 (2007).
[31]B. Bhushan, Appl. Opt. **24**, 1489 (1985).
[32]K. Abbas, Int. J. Appl. Sci. Eng. **3**, 135 (2005).
[33]B. T. Kimbrough, Appl. Opt. **45**, 4554 (2006).
[34]S. Karout, *Two-Dimensional Phase Unwrapping*, Ph.D. dissertation, Liverpool John Moores University, 2007.
[35]Y. Kaganovskii, I. Antonov, F. Bass, M. Rosenbluh, and A. Lipovskii, J. Appl. Phys. **89**, 8273 (2001).
[36]I. Antonov, F. Bass, Y. Kaganovskii, M. Rosenbluh, and A. Lipovskii, J. Appl. Phys. **93**, 2343 (2003).
[37]G. Stewart and P. J. R. Laybourn, IEEE J. Quantum Electron. **14**, 930 (1978).
[38]W. T. Coffey, Y. P. Kalmykov, and J. T. Waldron, *The Langevin Equation*, 2nd ed. (World Scientific, Singapore, 2004).
[39]M. K. Choudhary and R. M. Potter, "Heat transfer in glass-forming melts," in *Properties of Glass-Forming Melts* (Taylor &Francis, London, 2005).
[40]B. D. Guenther, *Modern Optics* (Wiley, New York, 1990).
[41]R. W. Boyd, *Nonlinear Optics* (Academic, New York, 1992).
[42]J. Jost, *Partial Differential Equations* (Springer, New York, 2007), Vol. 10.
[43]S. Larsson and V. Thomée, *Partial Differential Equations With Numerical Methods* (Springer-Verlag, Berlin Heidelberg, 2003).
[44]J. Shelby, *Introduction to Glass Science and Technology*, 2nd ed. (The Royal Society of Chemistry, Cambridge, 2005).
[45]L. C. Burmeister, *Convective Heat Transfer*, 2nd ed. (Wiley, New York, 1993), p. 107.
[46]See http://www.engineeringtoolbox.com/overall-heat-transfer-coefficient-d_434.html for information about overall heat transfer coefficient.
[47]*COMSOL Multiphysics Modeling Guide* (COMSO LAB, Los Angeles, 2008), Version 3.5.
[48]S. Kinumaki and T. Ito, Sci. Rep. Res. Tohoku Univ. A **8**, 60 (1956).
[49]A. L. Stepanov, V. N. Popok, D. E. Hole, and A. A. Bukharaev, Phys. Solid State **43**, 2192 (2001).